Penerbit Akademia Baru

Journal of Advanced Research in Micro and Nano Engineering

Journal homepage:
https://www.akademiabaru.com/submit/index.php/armne/index
ISSN: 2756-8210

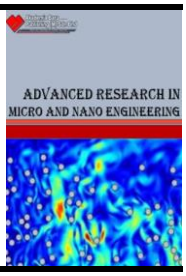

Comparative Study of Q-Switched Erbium Doped Fibre Laser with SWCNT-PVA Saturable Absorber of Different Ratios

Ooi Wei Ling[1], Azura Hamzah[1,*], Norliza Mohamed[2], Nur Najahatul Huda[3], Ahmad Haziq Aiman Rosol[1], Kawther M. Mustafa[1], Mahroof Mohamed Mafroos[4]

[1] Malaysia-Japan International Institute of Technology (MJIIT), Universiti Teknologi Malaysia, Jalan Sultan Yahya, 54100 Kuala Lumpur, Malaysia
[2] Razak Faculty of Technology and Informatics (RFTI), Universiti Teknologi Malaysia, Jalan Sultan Petra Yahya, 54100 Kuala Lumpur, Malaysia
[3] School of Electrical, Faculty of Engineering, Universiti Teknologi Malaysia, 81310 Johor Bahru, Johor, Malaysia
[4] Division of Electrical and Electronic, Telecommunication Engineering Technology, Institute Technology Universiti of Moratuwa, Sri Lanka

ARTICLE INFO

Article history:
Received 28 October 2023
Received in revised form 1 December 2023
Accepted 5 January 2024
Available online 29 February 2024

Keywords:
Q-switched; erbium doped fibre (EDF); SWCNT-PVA; saturable absorber

ABSTRACT

This paper intends to compare the performance parameters of passive Q-switched erbium-doped fibre laser (EDFL) ring cavity configuration by employing SWCNT-PVA as a saturable absorber (SA). The single-wall carbon nanotube-polyvinyl alcohol (SWCNT-PVA) SA thin film fabricated by drop-casting technique is physically characterised to understand its surface morphology and thickness. The laser diode (LD) characterisation is attained to understand the attributes of LD before inserting the SWCNT-PVA into the ring cavity. The SWCNT-PVA SA of ratios 1:1, 3:2 and 2:3 is inserted into the cavity for analysis and comparison with each other. The pulses obtained from the Q-switched laser show that SWCNT-PVA SA of ratio 2:3 is the best SA as it possesses excellent power related parameters of the highest output power of 3.45 mW and highest pulse energy of 36.12 nJ with its moderate repetition rate of 96.25 kHz and pulse width 4.76 μs. The envisaged laser is presumed to have representational implications throughout fibre optic sensing, biosensors, range finding, and other fields for better possible prospects.

1. Introduction

In various applications of fibre lasers, for instance, micromachining, meteorology, laser cosmetics surgery, military, light detecting and ranging (LiDAR), telecommunication, nanotechnology, biomedical and chemical sensing, extensive instantaneous energy as compared to those supplied by continuous wave (CW) fibre lasers are requisitioned for the enhancement of light interaction with matters [1-8]. Hence, a Q-switched fibre laser that can generate a gigantic pulse in a transient time by either active or passive technique is endorsed comprehensively [9,10].

Compared to the active technique that requisites an external modulator, for instance, a mechanical, acousto-optic, or an electro-optic modulator to trigger a pulse by modulating the cavity losses, passive Q-switched fibre lasers have been an object of research due to its easy and

* *Corresponding author.*
E-mail address: azurahamzah@utm.my

https://doi.org/10.37934/armne.16.1.85101

straightforward accessible operation, determining stability which alludes to sophisticated accomplishments by the implementation of saturable absorbers (SA) [11-15]. One of the most significant discussions in passive Q-switched fibre lasers is its self-starting feature of spontaneously rectifying the losses in the cavity to attain a high repetition rate with nanoseconds short pulses periphrastically [16,17].

In a laser cavity, SA plays the role of a nonlinear optical medium that enhances the optical intensity of Q-switched fibre laser by enclosing the optical source in the fibre core and lowering the losses [18]. Moreover, previous studies have reported SA possessing favourable dominance in constructing and shaping the generated pulse [19]. SA is the study interest as the employment of miscellaneous materials with different characteristics in terms of modulation depth, saturable and non-saturable losses, saturable fluence, recovery time and damage threshold will generate the optical pulses with peculiar parameters [20].

In past decades, a nonlinear SA mirror, namely the semiconductor absorber mirror (SESAM) was the most extensively utilised SA. Conventionally, the key factor of the implementation of SESAM in Q-switched fibre lasers is due to its nonlinearity and precisely adjustable saturable absorption parameters [21]. Despite its benefits, SESAM has a number of problems in its application. The exploration of SESAM as SA for Q-switched fibre lasers encountered bottlenecks owing to intricate fabrication, restricted operational wavelength, and exorbitant costs [22]. Accordingly, the current research trend shifts towards alternative SA materials with greater achievement and reasonably low-prices.

Several attempts had been made to substitute SESAM with graphene nanomaterials as its exclusive honeycomb lattice structure which is composed of atomic thick sp^2 hybridised carbon enlightens electron mobility [23]. The striking features of graphene enacted as a zero-gap semiconductor with overlapping valance and conduction bands due to the bonding (π) and antibonding (π^*) orbital besides the lattice mislocating impediment and crystal inadequacy at high temperatures managed to carry it out as an auspicious SA with preferable performance [24-26].

Nonetheless, research has consistently shown that graphene accrued some concerns over modulation depth, light-matter interaction, and non-saturable losses [27]. The attainment of graphene in Q-switching pulse generation leads to two directions of SA materials:

i. carbon-based nanomaterials, for example, single-wall carbon nanotubes (SWCNT) and multi-wall carbon nanotubes (MWCNT)
ii. graphene-like 2-dimensional (2D) nanomaterials, such as transition metals (TMs), transition metal oxides (TMOs), transition metal dichalcogenides (TMDs), black phosphorus (BP), and metal nanoparticles [28-34].

This paper will focus on the former. SWCNT is a rolled-up graphene nanosheet by elemental tight-binding approximation accompanied by excellent nonlinear properties, modulation depth, saturable absorption, and optical absorption [35-37]. With the employment of SWCNT SAs, the research work attempts to observe the Q-switched pulse train from the perspective of:

i. temporal parameters which are pulse repetition rate and pulse width
ii. power-related parameters, which are output power and pulse energy corresponding to the aspects impacting the Q-factor

$$Q = \frac{2\pi f_o \varepsilon}{P} \quad (1)$$

Se where f_o is the resonant frequency, ε is stored energy in the cavity, and $P = -dE/dt$ is the power dissipated [38].

In this paper, the SWCNT-PVA SA thin films of 3 different ratios of 1:1, 3:2 and 2:3 is fabricated through the drop-casting technique by utilising the PVA as the host polymer. The SWCNT-PVA SAs fabricated are then undergone physical characterisation for the purpose to understand their atomic ratios, distribution, and atomic arrangements through their thicknesses and surface morphologies. Then, the SWCNT-PVA SAs are installed into the Q-switched erbium-doped fibre laser ring cavity for determining and analysing their performance through the optical spectra and parameters of pulses generated, which are repetition rate, pulse width, output power and pulse energy and compared among different ratios.

2. Methodology

This section mainly discusses the fabrication and characterisation of the saturable absorber (SA), the pump characterisation of the laser diode and configuring of the Q-switched erbium-doped fibre laser ring cavity.

2.1 Fabrication of Saturable Absorber

Figure 1 illustrates the SA fabrication of single-walled carbon nanotube (SWCNT) with polyvinyl alcohol (PVA), the host material that possesses non-hazardous characteristics, marvellous compatibility, stability and near zero optical absorption through an effective and straightforward drop-casting technique, one of the practical ways to form an SWCNT-PVA SA thin film with notable tensile strength and ability to endure an energetic laser source in the laser ring cavity.

2.5mg of sodium dodecyl sulphate (SDS) powder is weighed with an electronic balance (OHAUS, AX324) and agitated with 250ml of deionised (DI) water thoroughly by the use of a hot-plate stirrer (DATHAN SCIENTIFIC, MSH-20D) at the stirring speed of 360 rpm and temperature of 200 °C for an hour to obtain the SDS solution which serves as an agent to breakdown and averagely distribute the SWCNT. For the preparation of SWCNT solution, 40mg of SWCNT is measured and stirred with the appropriate 40ml SDS solution for 24 hours before undergoing an ultrasonication bath with a sonicator (FISHERBRAND, FB15050) at ultrasonic frequencies (≥20kHz) for the extraction of SWCNT compound.

PVA solution is adapted by mixing 1 g of PVA powder and 120 ml of DI water stirred entirely by using the hot-plate stirrer for another 24 hours. In accordance with the ratios of SWCNT and PVA, which are 1:1, 3:2 and 2:3 respectively, different volumes of SWCNT and PVA solutions are being infused into each of the 5 ml Petri dishes as shown in Table 1 for the solidification process of the SA thin film.

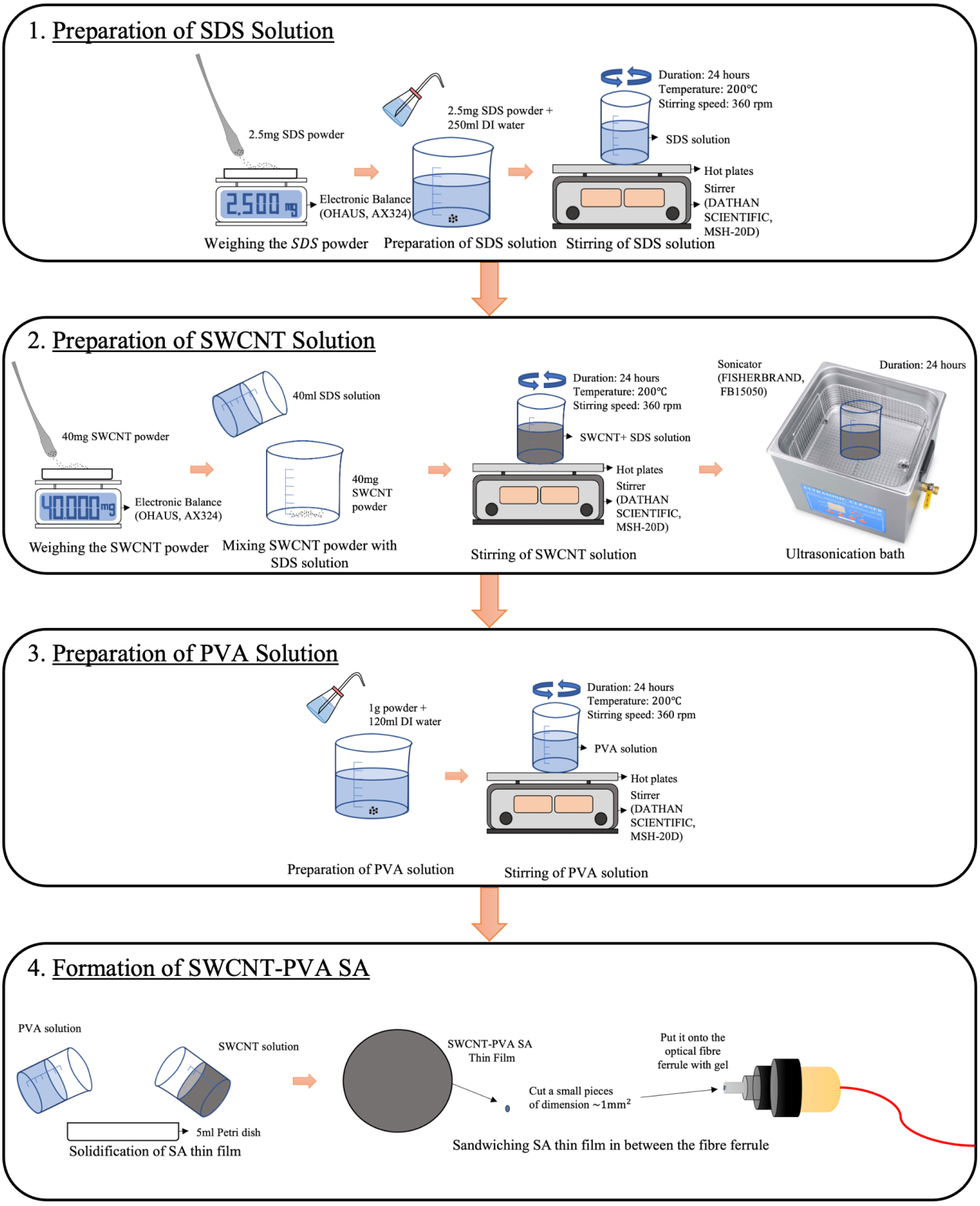

Fig. 1. Fabrication process of SWCNT-PVA SAs thin film using the drop-casting technique

The selection of these ratios of SWCNT-PVA SA relies on the various attempts to determine the ratios with better performance in its temporal and power-related parameters. Dry SWCNT-PVA SA thin films of ratios 1:1, 3:2 and 2:3 with a diameter of around 30 mm are fabricated.

In this work, the SWCNT-PVA SA thin films are incised into an approximately 1 mm^2 small piece and sandwiched independently in between the optical fibre ferrule facets which are connected to

the ring cavity configuration for the observation of performance parameters of each thin film respectively.

Table 1
The volume of SWCNT and PVA solutions concerning their ratios

Ratios	SWCNT solution (ml)	PVA solution (ml)
1:1	2.5	2.5
3:2	3.0	2.0
2:3	2.0	3.0

2.2 Physical Characterisation of Saturable Absorber

Before the utilisation of thin film as SA in the Q-switching ring cavity configuration, physical characterisation is done to identify the distribution of the SWCNT nanomaterial on the thin film through the thickness, surface morphology and chemical composition examinations. Thus, the availability of the fabricated SWCNT-PVA SA is authenticated with their atomic ratios, distribution, type and arrangement.

2.2.1 Thickness

The thickness of the SWCNT-PVA SA thin films is visualised in 3-dimensional (3D) images recorded through a 3D measuring laser microscope (OLYMPUS LEXT, OLS4100). The SA thin films of different ratios are sliced into specimens and located on a microscope slide (26x76x1.3±0.2 mm) with 200x magnification to obtain sharp and clear 3D images on a micrometre-scale. The 3D graph with x, y, and z axes and thickness profile of each ratio of SWCNT-PVA SA thin film is observed.

2.2.2 Surface morphology

To ensure the SWCNT is homogeneously distributed in the PVA, the surface morphology of SWCNT-PVA surface thin film is characterised by FESEM acronym for field emission scanning electron microscope (JEOL, JSL-7800F) at 10000x magnification with sub-1µm ultra-high resolution without distortion. The fine SWCNT-PVA thin film surfaces are analysed at low electron energy with a lower electron detector (LED) of FESEM.

2.3 Pump Characterisation of Laser Diode

The configuration as detailed in Figure 2 is appropriated for laser diode (LD) characterisation. A 980 nm LD source (Q-photonics, QFLD-405-20S) located in a benchtop laser controller (GOOCH & HOUSEGO, EM595) assumes the role of an amplifier and power booster to pump the laser cavity. The input power is then pumped through a 980/1550 nm wavelength division multiplexer (WDM 980/1550nm) which multiplexes optical signals of dissimilar frequencies configuration. The input pump power in the range of 0 to 350 mA is then characterised by an optical power meter (OPM; Thorlabs, PM100D) to obtain the laser diode power in terms of milliwatts (mW). A graphical data is illustrated and a curve fitting equation is investigated.

Fig. 2. Configuration of laser diode characterisation

2.4 Q-Switched EDFL Ring Cavity Configuration

Figure 3 illustrates the laser cavity configuration constructed by organising and splicing the optical components laboriously and precisely using an optical splicer (FUJIKURA, 70S+) into a ring cavity. The availability of the ring cavity configuration is checked by utilising fibre inspection scope (THORLABS, FS201).

The 980 nm LD (Q-photonics, QFLD-405-20S) located in the benchtop laser controller (GOOCH & HOUSEGO, EM595) acting as a unidirectional power source is connected to the 980 nm port of 980/1550 nm WDM which apportions the wavelength-dependent laser light in 980 nm and 1550 nm ports, letting the light be transmitted through the 1.7 m erbium-doped fibre (EDF; NUFERN, SM-ESF-7/125) with 8.8±1.0 μm mode field diameter (MFD) at 1550 nm, a cut-off wavelength at 1400±60 nm, core numerical aperture of 0.150, and 55.0±5.0 dB/m core absorption at near 1530 nm, which perform as the active gain medium doped with erbium ions.

In this experiment, a polarisation-independent unidirectional isolator is utilised to prevent undesired flow back of propagated light which may damage the LD and engender back-reflection inside the laser cavity. A 95:5 ratio optical coupler lets 95% of the optical signal toward an FC/PC optical fibre ferrule and is linked to the 1550 nm port of WDM while the remaining 5% is coupled out for measurement intent.

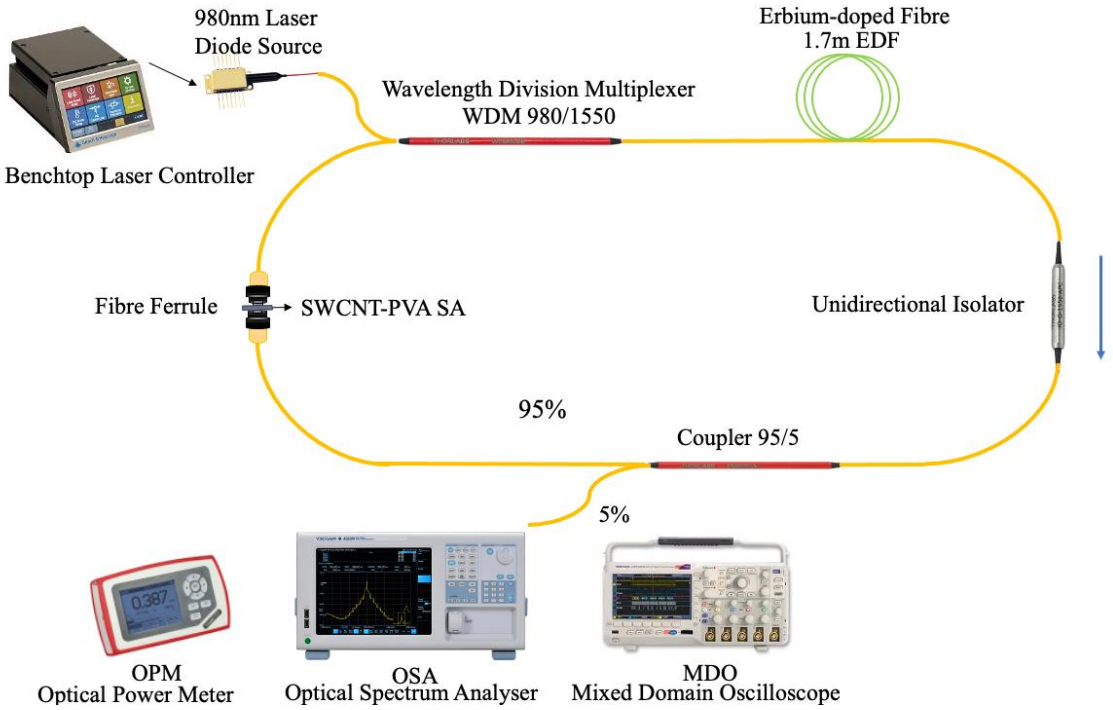

Fig. 3. Q-switched EDFL ring cavity configuration

For the study of different ratios of SWCNT-PVA SA as a Q-switcher, the fabricated SWCNT-PVA SA thin film is cleaved into around 1 mm^2 and positioned in between the end facets of FC/PC optical fibre ferrules. The 5 % light signal coupled out is then connected to an optical spectrum analyser (OSA; Yokogawa, AQ6370D) for analysing the optical spectrum of SWCNT-PVA SAs of different ratios.

Subsequently, the coupled signal is attached to a mixed domain oscilloscope (MDO; TEKTRONIX, MDO3024) to examine the temporal parameters of the pulse train generated, which are pulse repetition rate f_R and pulse width Δt. The power-related parameters; the optical output power P_{avg} is examined by the utilisation of optical power meter (OPM; THORLABS, PM100D), while the pulse energy U is determined by calculation as stated

$$U = \frac{P_{avg}}{f_R} \tag{2}$$

The performance parameters are compared to determine the ideal ratio for achieving the desired condition of having relatively high output power, high repetition rate, high pulse energy, and short pulse width.

3. Results and Discussion

3.1 Physical Characterisation of Saturable Absorber

3.1.1 Thickness

Referring to the (i) 3D graph and (ii) thickness profile as shown in Figures 4 (a), (b) and (c), the thickness of SWCNT-PVA SA thin films of ratios 1:1, 3:2, and 2:3 is measured to be 15.322µm, 31.389µm and 27.371µm respectively. From the data obtained, it is apparent that the thickness of SWCNT-PVA SA thin films is meticulously related to their ratios and volumes of SWCNT solution being used.

Interestingly, the ratio and volume of SWCNT solution are significantly in a directly proportional relationship with the average thickness of the thin films fabricated. Retrieved from the thickness, the correctness and preciseness of the ratios and volumes of the SWCNT solution in thin film fabrication are validated.

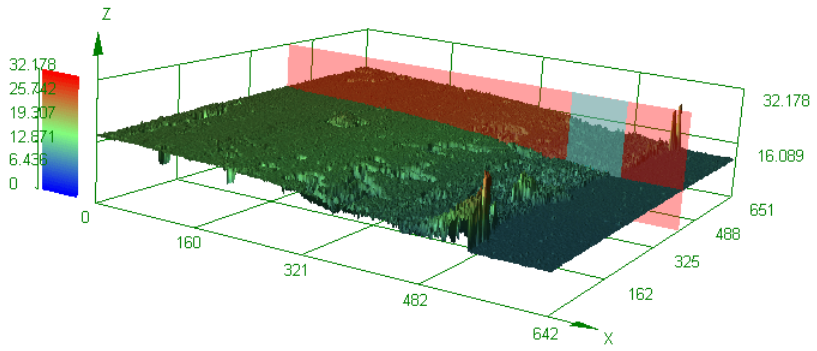

(a) (i)

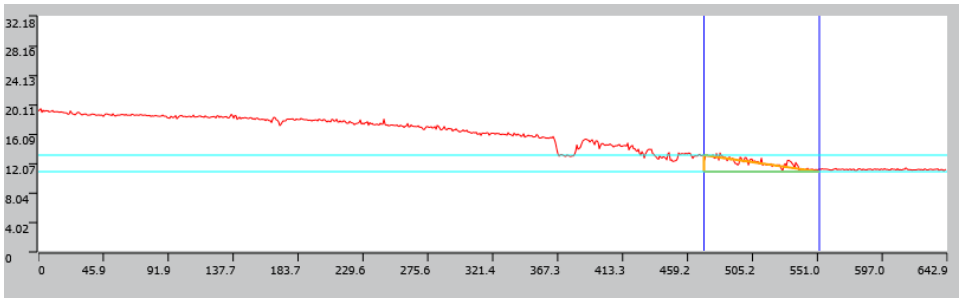

(a) (ii)

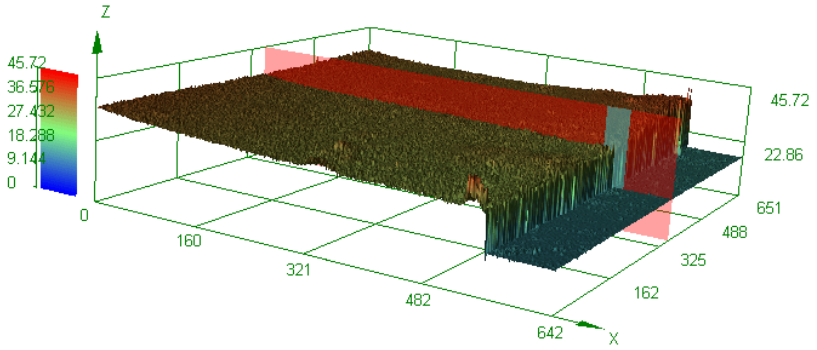

(b) (i)

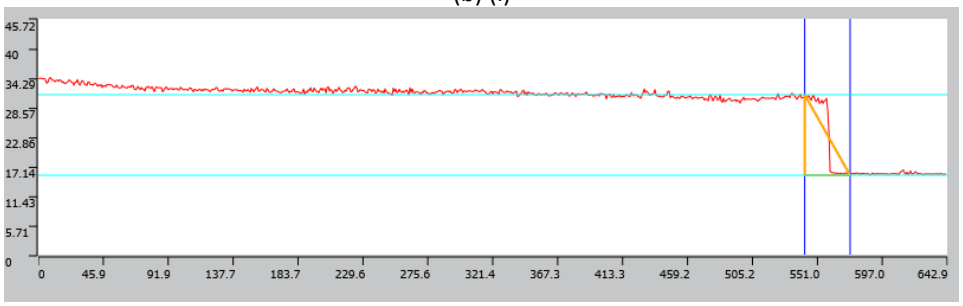

(b) (ii)

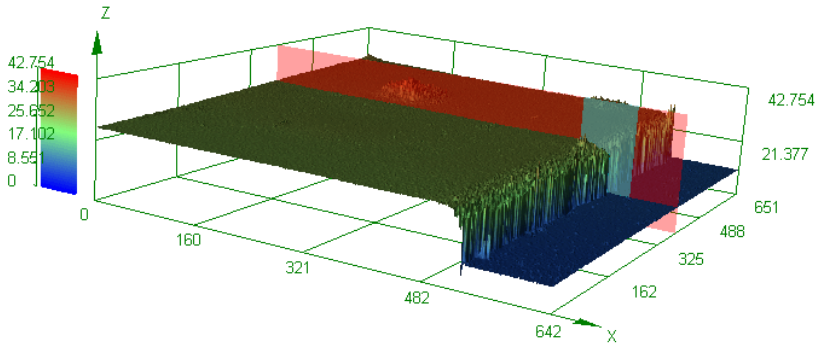

(c) (i)

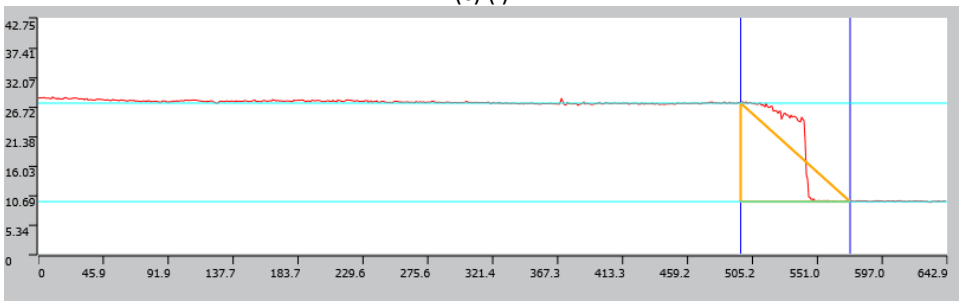

(c) (ii)

Fig. 4. (i) 3D graph and (ii)thickness profile of SWCNT-PVA thin film of ratio (a)1:1; (b)3:2 and (c)2:3

3.1.2 Surface morphology

Figure 5 depicted the surface morphologies of SWCNT-PVA SA thin films of ratios 1:1, 3:2 and 2:3 respectively. As shown in Figure 5, the lustrous, detritus and delaminated carbon flakes are dispersed adequately and firmly on the nanomaterial surfaces without any contamination. The findings demonstrated that all of these thin films are firmly distributed by only SWCNT and PVA, disregarding any other nanomaterials at the micro- to nano-scale.

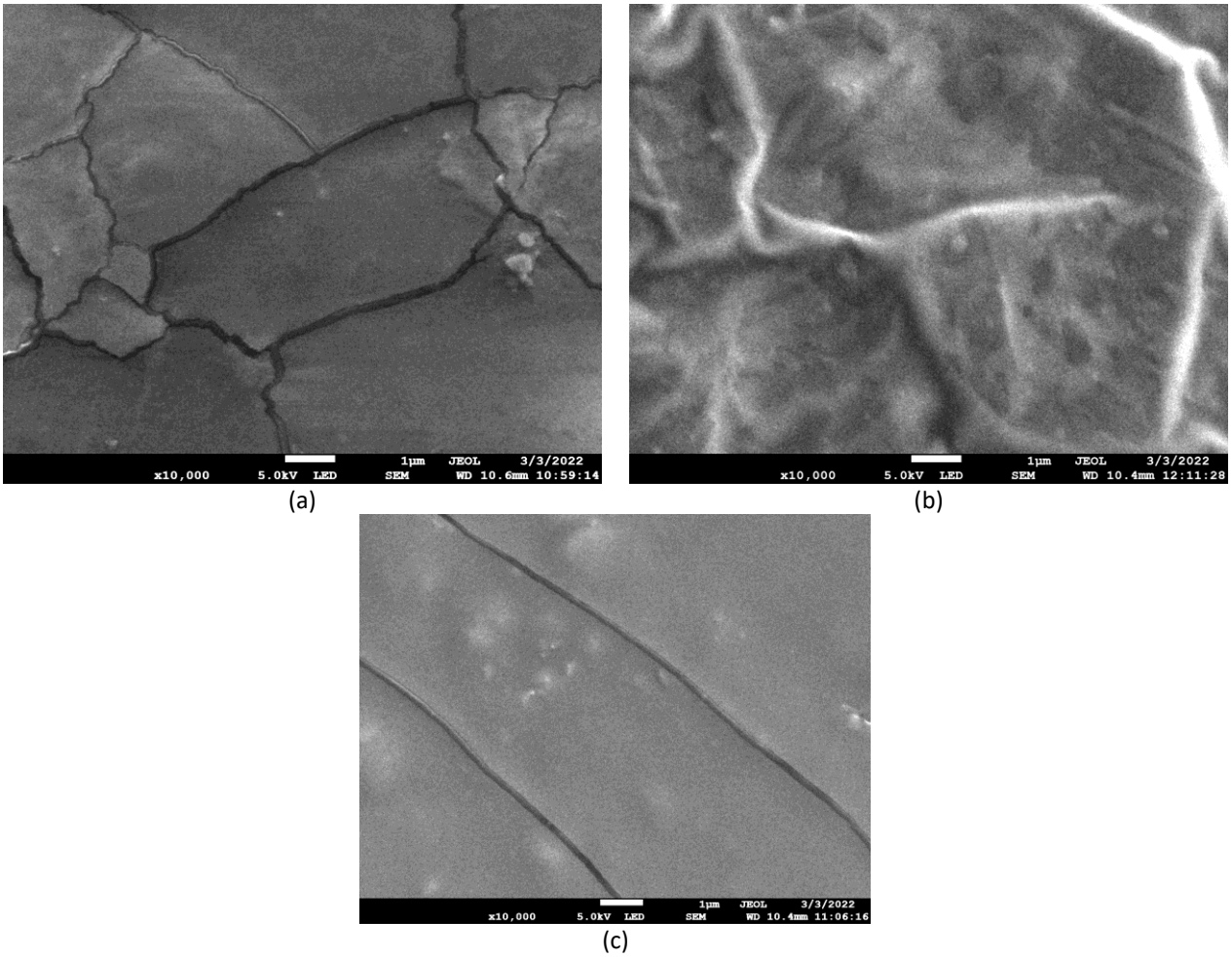

Fig. 5. Surface morphology of SWCNT-PVA thin film of ratio (a)1:1; (b)3:2 and (c)2:3

3.2 Pump Characterisation of Laser Diode

Figure 6 exemplified the pump characterisation of pump power in mW after WDM. As scrutinised from the figure, there is no output power until the pump power supplied is greater than 40 mA. At the back of it, a stable operational wavelength triggers at 40 mA.

The range of the stable operational wavelength is indicated by linear increases in mW of pump power against mA. The highest stable pumping to be obtained is at the pump power of 350 mA. Hence, the pump power range can be adjudged as 40 mA to 350 mA (3.5 mW to 177.6 mW) to achieve pulse stability.

Nevertheless, the pump characterisation of pump power after WDM is further explained by the curve fitting equation below

$$y = 0.56161x - 18.96452 \quad (3)$$

where y represents the y-axis, LD power in milliwatts and x represents the x-axis, LD current in milliamperes. By this equation, the relationship between the current supply of the LD diode and the input pump power is demonstrated.

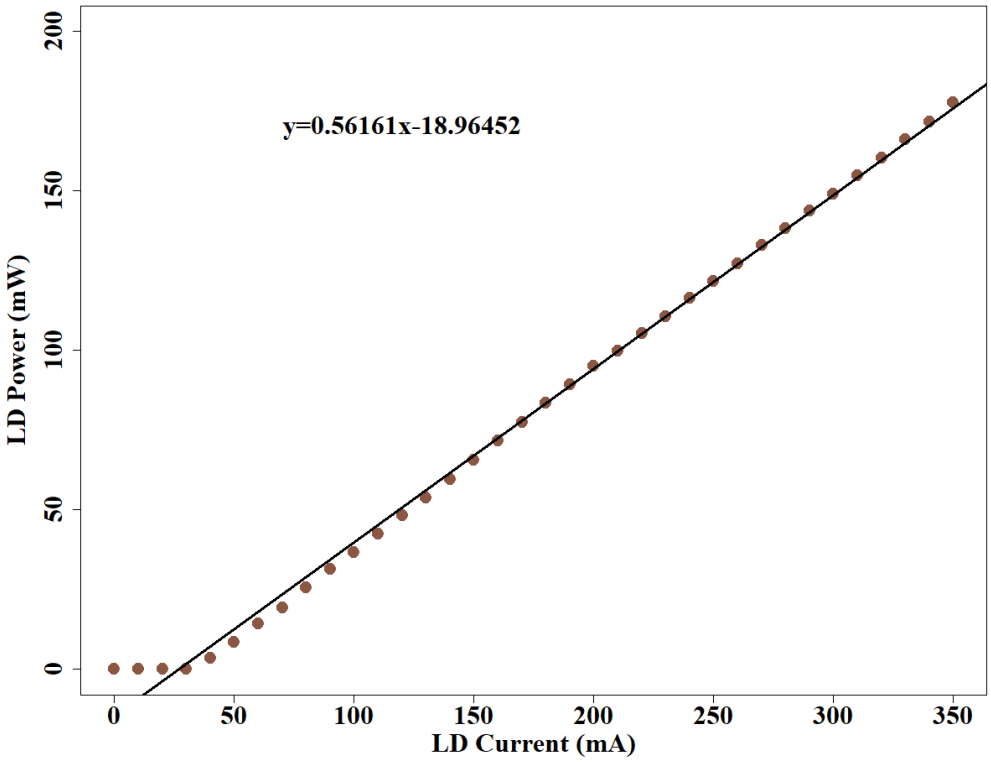

Fig. 6. Characterisation of pump power

3.3 Q-Switched EDFL Ring Cavity Configuration

The optical spectra are priorly compared to the laser ring cavity configuration without SA as a study control. The threshold pump power of the cavity without the insertion of SA is 14.73 mW, and 20.35 mW, 31.58 mW and 65.28 mW for the laser cavities with the insertion of SWCNT-PVA SAs of ratio 1:1, 3:2 and 2:3 in accordance as shown in Table 2.

These values indicated the incident pump powers to initiate the generation of lasers and ensure excellent performance in their output powers, power efficiencies, noise levels and stabilities. The higher threshold pump power also indicated the higher attainable output power. In this manner, the SWCNT-PVA SA of ratio 2:3 tends to possess the greatest output power and power efficiency, significantly low noise level, and high stability as it has the greatest threshold pump power.

Nonetheless, there is a range for each laser cavity to perform its stable pulse train. This range is from 20.35 mW to 98.97 mW for SWCNT-PVA SA with the ratio of 1:1; from 31.58 mW to 149.52 mW for SWCNT-PVA SA with the ratio of 3:2; and, from 65.28 mW to 177.60 mW for SWCNT-PVA SA with the ratio of 2:3. The Q-switching pulses are not stable and are undermined henceforward when the pump powers are in excess of these ranges.

Table 2
Comparison of centre wavelengths and signal level of Q-switched fibre laser configuration with different ratios of SWCNT-PVA SAs

Ratio of SWCNT-PVA SA	Threshold pump power (mW)	Centre wavelengths (nm)	Signal level (dBm)
Without SA	14.73	1561.75	-11.13
1:1	20.35	1558.29	-29.10
3:2	31.58	1558.41	-19.38
2:3	65.28	1557.46	-2.68

The Q-switched fibre laser ring cavities constituted by SWCNT-PVA of different ratios are then set to their maximum tuneable pump power for observing the optical spectra as illustrated in Figure 7. The central wavelength of these laser cavity configurations is observed to be stationed at the conventional band (C-band) with the adoption of EDF as the gain medium because the emission wavelength of EDF is around 1550nm [39]. The laser with the emission spectrum at this wavelength range is suitable for being utilised in optical communication [40].

The centre wavelength is observed to be 1561.75 nm with the signal level at -11.13 dBm as case-control, meanwhile, the centre wavelength and noise level of the laser cavities with the insertion of SWCNT-PVA SAs should be less than 1561.75 nm and greater than -11.13dBm for enhancing the fibre laser configuration. The centre wavelengths and signal levels of Q-switched fibre laser with SWCNT-PVA SAs of ratios 1:1, 3:2 and 2:3 is 1558.29 nm at -29.10 dBm, 1558.41 nm at -19.38 dBm, 1557.46 nm at -2.68 dBm correspondingly.

Based on this result, the centre wavelengths of all the cavities are indicated to be significantly left-shifted, which means that higher emission energies can be attained as explained by the combination of Plank's law and the equation of light speed [41]

$$E = h(\frac{c}{\lambda}) \tag{4}$$

where E is the emission energy of photons, h is the Plank's constant, c is the speed of light, and λ is the operational wavelengths of the Q-switched fibre laser in accordance. Eq. (4) clearly stated that E is in an inversely proportionated relationship with λ, which means the decrease in λ brings to the increase in emission energy. From this perspective, the results of 3 different ratios of SAs are acceptable.

From the insight from the signal level, the one and only Q-switched fibre laser cavity provided greater than -11.13 dBm is SWCNT-PVA SA of ratio 2:3. The notable greatness in signal value in the SWCNT-PVA SA of ratio 2: 3 means higher output power is attainable. The Q-switched fibre laser ring cavity configuration constructed with SWCNT-PVA SA of ratio 2:3 is the best SA ratio as it has a significant left-shifted centre wavelength and excellent signal level.

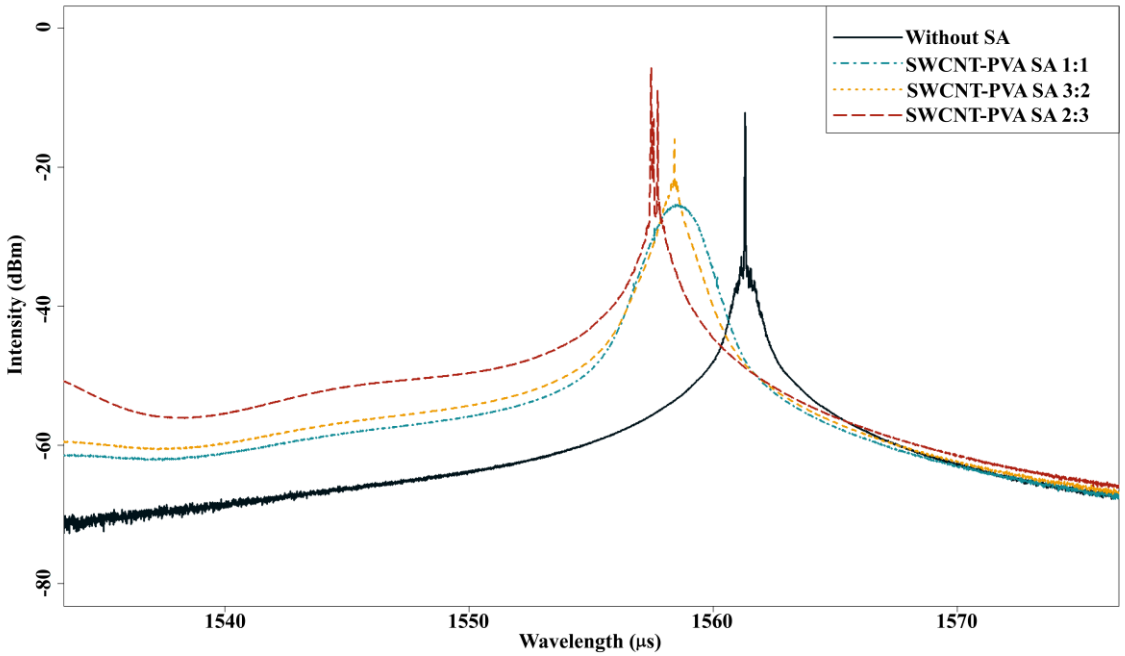

Fig. 7. Optical Spectra of Q-switched EDFL for SWCNT-PVA SA thin films with different ratios

In general, there are 2 key factors affecting the passive Q-switched fibre laser to be commercialised:

i. high speed, so 'eye-safe' short pulses will be produced
ii. high power, so the production can be increased and losses can be reduced with the same amount of pump power supplied.

Hence 2 types of parameters are indicated in this experiment, which are:

i. temporal parameters
ii. power-related parameters. Temporal parameters studied the nature of the pulses generated through repetition rate and pulse width; Power-related parameters study the output power and pulse energy.

3.3.1 Temporal parameters

3.3.1.1 Pulse repetition rate

Once the repetition rate of the passive Q-switched EDFL configuration was recorded, particularly in comparison to the repetition rate of the SWCNT-PVA SA of different ratios, as shown in Figure 8(a), the ratio of 3:2 is acknowledged as the ratio with the highest repetition rate of 194.2 kHz, which was approximately twice that of the other ratios, denoting that more gain was implemented to saturate the SA [42].

While visually inspecting the passively Q-switched EDFL with SWCNT-PVA SA of ratios 1:1 and 2:3, a higher repetition rate of 96.25kHz is attained by the passively Q-switched fibre laser with SWCNT-PVA SA of ratio 2:3 since it was inaugurated with a comparatively greater input pump power, which was in direct proportion to the repetition rate. Nevertheless, there is significant increasing curve for the pulse repetition rate of ratio 1:1 at pump power 59.6mW due to thermal change [43].

3.3.1.2 Pulse width

If the passive Q-switched EDFL with SWCNT-PVA SA of different ratios are compared, as shown in Figure 8(b), the passively Q-switched fibre laser with SWCNT-PVA SA of ratio 3:2 attained a minimum pulse width of 2.39μs at the threshold power of 149.52 mW. The lower the lowest attainable pulse width was obligatory.

As the smallest value of minimum pulse width is procured, the pulse will be more stable since such greater modulation depth will maximise the incident light absorption. On the other hand, the minimum achievable pulse width, produced little resemblance because it was constrained to micro-scale. Similar to the repetition rate, at 59.6mW, a remarkable decrement in pulse width is observed in ratio 1:1 as the number of pulses emitted per second is increase, hence the pulse duration is decrease in particular.

3.3.2 Power-related parameters
3.3.2.1 Output power

Figure 8(c) reveals a comparison of the output power of the passive Q-switched EDFL with SWCNT-PVA SA in ratios of 1:1, 3:2 and 2:3. Since the input pump power was proportional to the output power, the SWCNT-PVA SA with a ratio of 2:3 was presumably one with the highest output power.

3.3.2.2 Pulse energy

Referring to Figure 8(d), which measures up the pulse energy of passive Q-switched EDFL of different ratios, the ratio of 2:3 achieved the pulse energy that was all time greater than the other ratios within its range for resolving pulse stability and maximum pulse energy of 36.12 nJ at the input power of 171.7 mW as the pulse energy was directly proportional to the output power and inversely proportional to the pulse repetition rate.

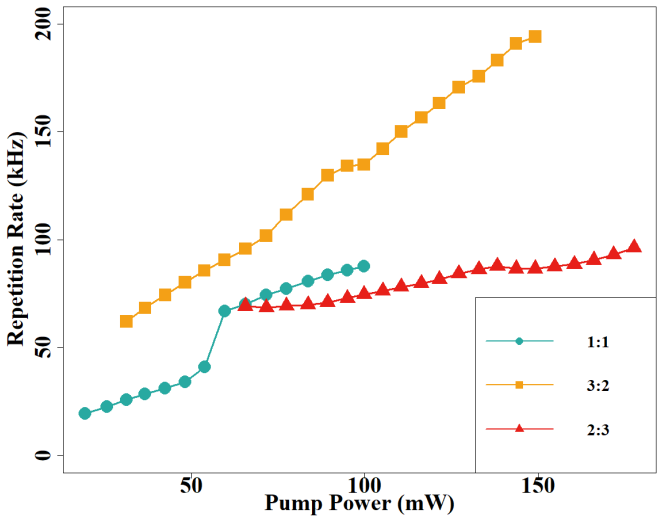

(a)

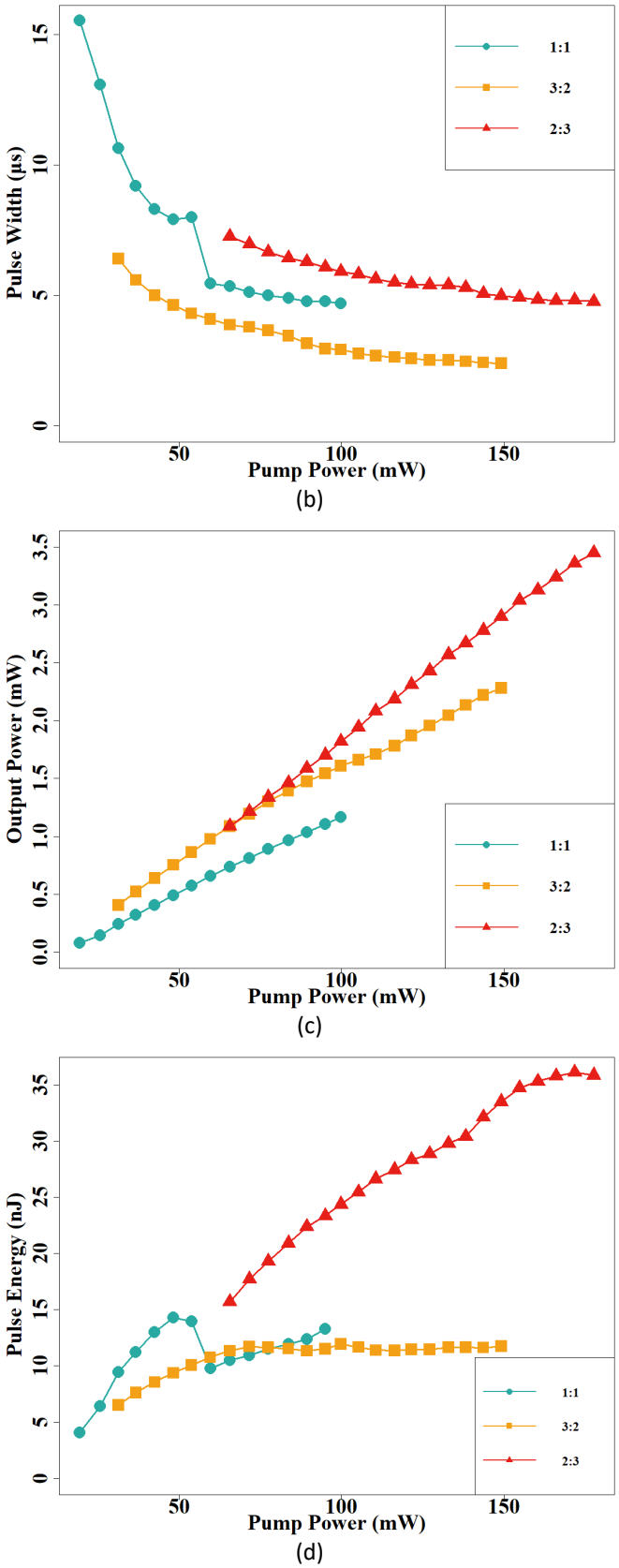

Fig. 8. Comparison study of Q-switched EDFL of (a) repetition rate; (b) pulse width; (c) output power; and (d) pulse energy

Upon analysing and comparing, the passively Q-switched fibre laser with SWCNT-PVA SA of ratio 2:3 was preferred as the one with the best performance as it retrieved the greatest output power and pulse energy with a markedly short pulse width, notwithstanding its repetition rate to be lower than expected. At 59.6 mW, a phenomenal of decreasing in repetition rate is determined as it varies inversely to the pulse energy which shows an increasing trend.

Generally, the SWCNT-PVA SA of ratio 1:1, 3:2 and 2:3 is suitable to be utilised as Q-switcher as three of them possess excellent output values. The SWCNT-PVA SA of ratio 2:3 is determined as the best ratio as it reached the divide output power and pulse energy which is the vital parameters to be commercially competitive to other SA nanomaterials with tolerable pulse repetition rate and pulse width.

4. Conclusions

Ultimately, the passive Q-switched EDFL is optimised by using SWCNT-PVA SA in the affiliated: 1:1, 3:2, and 2:3 ratios. The SWCNT-PVA SA of ratio 2:3 exhibits the greatest repetition rate of 96.25 kHz, and the maximum output power of 3.45mW, the highest pulse energy of 36.12 nJ, and the lowest pulse width of 4.76 μs, demonstrating the desired Q-factor. To enable success in the future, the proposed laser will have expressive functionalities in a range of disciplines.

Acknowledgement

The authors gratefully acknowledge the financial support of the Ministry of Higher Education Malaysia for their encouragement and grant support under the Fundamental Research Grant Scheme (FRGS/1/2020/TK0/UTM/02/46).

References

[1] Rosol, A. H. A., N. F. Zulkipli, R. Apsari, M. Yasin, and S. W. Harun. "Q-switched neodymium-doped fiber laser with a gold nanoparticle saturable absorber." *Microwave and Optical Technology Letters* 64, no. 7 (2022): 1302-1309. https://doi.org/10.1002/mop.33254

[2] Ismail, Mohd Afiq, Sulaiman Wadi Harun, Harith Ahmad, and Mukul Chandra Paul. "Passive Q-switched and mode-locked fiber lasers using carbon-based saturable absorbers." *Fiber Laser* (2016): 43-69. https://doi.org/10.5772/61703

[3] Awang, Noor Azura, Nor Syuhada Aziz, Atiqah Nabieha Azmi, Fatin Shaqira Hadi, and Zahariah Zakaria. "Experimental and numerical comparison Q-switched fiber laser generation using graphene as saturable absorber." In *MATEC web of conferences*, vol. 150, p. 01009. EDP Sciences, 2018. https://doi.org/10.1051/matecconf/201815001009

[4] Wang, Pan, and Vittorio Scardaci. "Passively Q-switched Yb-doped fiber laser based on Ag nanoplates saturable absorber." In *EPJ Web of Conferences*, vol. 243, p. 14004. EDP Sciences, 2020. https://doi.org/10.1051/epjconf/202024314004

[5] Muhammad, Ahmad Razif, Rozalina Zakaria, Muhammad Taufiq Ahmad, Pengfei Wang, and Sulaiman Wadi Harun. "Pure gold saturable absorber for generating Q-switching pulses at 2 μm in thulium-doped fiber laser cavity." *Optical Fiber Technology* 50 (2019): 23-30. https://doi.org/10.1016/j.yofte.2019.02.010

[6] Chen, Yujin, Jianhua Huang, Yanfu Lin, Xinghong Gong, Zundu Luo, and Yidong Huang. "Stable passively Q-switched 1537 nm Er: Yb: Lu2Si2O7 pulse microlaser with peak output power higher than 10 kW at 1–2 kHz." *Optics & Laser Technology* 155 (2022): 108392. https://doi.org/10.1016/j.optlastec.2022.108392

[7] Bonan, Paolo, Andrea Bassi, Nicola Bruscino, Emiliano Schincaglia, Maria Gavrilova, Michela Troiano, and Alice Verdelli. "Combined pulsed dye laser and Q-switched Nd: YAG laser intraumatic facial tattoo removal: a case series." *Dermatologic Therapy* 32, no. 5 (2019): e13069. https://doi.org/10.1111/dth.13069

[8] Silvestri, Martina, Luigi Bennardo, Elena Zappia, Federica Tamburi, Norma Cameli, Giovanni Cannarozzo, and Steven Paul Nisticò. "Q-switched 1064/532 nm laser with picosecond pulse to treat benign hyperpigmentations: A single-center retrospective study." *Applied Sciences* 11, no. 16 (2021): 7478. https://doi.org/10.3390/app11167478

[9] Yuan, Junjie, Guowei Liu, Yi Xin, Fei Xing, Kezhen Han, Wenfei Zhang, Fang Zhang, and Shenggui Fu. "Passively Q-switched modulation based on antimonene in erbium-doped fiber laser with a long term stability." *Optical Materials* 118 (2021): 111256. https://doi.org/10.1016/j.optmat.2021.111256

[10] Sompo, Justice Mpoyo, Kaboko Jean-Jacques Monga, Johan Meyer, and Sune Von Solms. "Peak Power and Pulse Shape of an Active Q-Switched Fiber Laser Based on Overlap of Narrow Filters." In *2021 IEEE AFRICON*, pp. 1-6. IEEE, 2021. https://doi.org/10.1109/AFRICON51333.2021.9570863

[11] Shen, Yanlong, Yousheng Wang, Feng Zhu, Lianying Ma, Liu Zhao, Zhengge Chen, Hao Wang, Chao Huang, Ke Huang, and Guobin Feng. "200 μJ, 13 ns Er: ZBLAN mid-infrared fiber laser actively Q-switched by an electro-optic modulator." *Optics Letters* 46, no. 5 (2021): 1141-1144. https://doi.org/10.1364/OL.418950

[12] Lau, Kuen Yao, Alexander Pyymaki Perros, Diao Li, Maria Kim, and Zhipei Sun. "Scalable graphene electro–optical modulators for all-fibre pulsed lasers." *Nanoscale* 13, no. 21 (2021): 9873-9880. https://doi.org/10.1039/D0NR08784J

[13] Chen, Tenghui, Weichao Yao, Hiyori Uehara, Chunyang Ma, Muhammad Sohail, Chunxiang Zhang, Yanqi Ge, Dianyuan Fan, and Jun Liu. "High-peak-power and wavelength tunable acousto-optic Q-switched Er: ZBLAN fiber laser." *Japanese Journal of Applied Physics* 61, no. 4 (2022): 040902. https://doi.org/10.35848/1347-4065/ac58d5

[14] Ahmad, Harith, Siti Nabila Aidit, Shok Ing Ooi, and Zian Cheak Tiu. "Tunable passively Q-switched erbium-doped fiber laser with Chitosan/MoS2 saturable absorber." *Optics & Laser Technology* 103 (2018): 199-205. https://doi.org/10.1016/j.optlastec.2018.01.032

[15] Siddiq, Nur Abdillah, Wu Yi Chong, Yono Hadi Pramono, Melania Suweni Muntini, and Harith Ahmad. "C-band tunable performance of passively Q-switched erbium-doped fiber laser using Tin (IV) oxide as a saturable absorber." *Optics Communications* 442 (2019): 1-7. https://doi.org/10.1016/j.optcom.2019.02.068

[16] Zha, Songqing, Yujin Chen, Bingxuan Li, Yanfu Lin, Wenbin Liao, Yuqi Zou, Chenghui Huang, Zhanglang Lin, and Ge Zhang. "High-repetition-rate 1.5 μm passively Q-switched Er: Yb: YAl 3 (BO 3) 4 microchip laser." *Chinese Optics Letters* 19, no. 7 (2021): 071402. https://doi.org/10.3788/COL202119.071402

[17] Cannarozzo, Giovanni, Steven Paul Nisticò, Elena Zappia, Ester Del Duca, Eugenio Provenzano, Cataldo Patruno, Francesca Negosanti, Mario Sannino, and Luigi Bennardo. "Q-Switched 1064/532 nm Laser with Nanosecond Pulse in Tattoo Treatment: A Double-Center Retrospective Study." *Life* 11, no. 7 (2021): 699. https://doi.org/10.3390/life11070699

[18] Cheng, Chih-Hsien, and Gong-Ru Lin. "Carbon nanomaterials based saturable absorbers for ultrafast passive mode-locking of fiber lasers." *Current Nanoscience* 16, no. 3 (2020): 441-457. https://doi.org/10.2174/1573413715666191114150100

[19] Debdeep Jena "Lasers & Optoelectronics Lecture 25: Modulators and Saturable Absorbers (Cornell ECE4300 Fall 2016)." *YouTube.* YouTube, (2017). https://www.youtube.com/watch?v=dagC4l3G5Po&t=1502s

[20] Mu, Haoran, Yani Liu, Sudhakara Reddy Bongu, Xiaozhi Bao, Lei Li, Si Xiao, Jincheng Zhuang *et al.,* "Germanium nanosheets with dirac characteristics as a saturable absorber for ultrafast pulse generation." *Advanced Materials* 33, no. 32 (2021): 2101042. https://doi.org/10.1002/adma.202101042

[21] Gao, Xibao, Zhigang Zhao, Zhenhua Cong, Guanguang Gao, Aiguo Zhang, Honglong Guo, Gang Yao, and Zhaojun Liu. "Stable 5-GHz fundamental repetition rate passively SESAM mode-locked Er-doped silica fiber lasers." *Optics Express* 29, no. 6 (2021): 9021-9029. https://doi.org/10.1364/OE.414779

[22] Chen, Tenghui, Zhongjun Li, Chunxiang Zhang, Zhenhong Wang, Mulin Luo, Yuan Zhang, Yachao Wang, Quanlan Xiao, Han Zhang, and Jun Liu. "Indium selenide for Q-switched pulse generation in a mid-infrared fiber laser." *Journal of Materials Chemistry C* 9, no. 18 (2021): 5893-5898. https://doi.org/10.1039/D1TC00727K

[23] Shakaty, Aseel A., Jassim K. Hmood, and Bushra R. Mhdi. "Graphene-based saturable absorber for pulsed fiber laser generation." In *Journal of Physics: Conference Series*, vol. 1795, no. 1, p. 012048. IOP Publishing, 2021. https://doi.org/10.1088/1742-6596/1795/1/012048

[24] Dong, Li, Hongwei Chu, Ying Li, Shengzhi Zhao, Guiqiu Li, and Dechun Li. "Nonlinear optical responses of α-Fe2O3 nanosheets and application as a saturable absorber in the wide near-infrared region." *Optics & Laser Technology* 136 (2021): 106812. https://doi.org/10.1016/j.optlastec.2020.106812

[25] Speranza, Giorgio. "Carbon nanomaterials: Synthesis, functionalization and sensing applications." *Nanomaterials* 11, no. 4 (2021): 967. https://doi.org/10.3390/nano11040967

[26] Chatzidimitriou, Dimitrios, Dimitrios C. Zografopoulos, and Emmanouil E. Kriezis. "Graphene Saturable Absorber Mirrors for Silicon Photonic Platforms." *IEEE Photonics Journal* 14, no. 4 (2022): 1-8. https://doi.org/10.1109/JPHOT.2022.3188222

[27] Wang, Jiang, Guangying Li, Guodong Zhang, Jing Lv, Wei Zhang, Fangtong Guo, Yuanshan Liu, Guanghua Cheng, and Xuelong Li. "Mxene Ti3C2Tx Langmuir–Blodgett films as saturable absorber for near-infrared Q-switched laser." *Infrared Physics & Technology* 119 (2021): 103945. https://doi.org/10.1016/j.infrared.2021.103945

[28] Stoliarov, D. A., P. A. Itrin, D. A. Korobko, V. A. Ribenek, L. V. Tabulina, A. V. Sysa, and Yu P. Shaman. "Saturable absorber based on the fiber coupler coated by CNTs." *Optical Fiber Technology* 63 (2021): 102524. https://doi.org/10.1016/j.yofte.2021.102524
[29] Silva, Luís CB, and Carlos ES Castellani. "Recent progress in optical dark pulses generation based on saturable absorber materials." *Optical Fiber Technology* 64 (2021): 102560. https://doi.org/10.1016/j.yofte.2021.102560
[30] Noor, S. F. S. M., Nur F. Zulkipli, T. F. T. M. N. Izam, Harith Ahmad, Moh Yasin, and Sulaiman Wadi Harun. "Q-switched tunable fiber laser with aluminum oxide saturable absorber and Sagnac loop mirror." *Indian Journal of Physics* 95 (2021): 1887-1893. https://doi.org/10.1007/s12648-020-01867-4
[31] Ahmad, Harith, Nor Hidayah Abdul Kahar, Norazriena Yusoff, Muhamad Zharif Samion, Siti Aisyah Reduan, Mohammad Faizal Ismail, Leonard Bayang, Yu Wang, Siyi Wang, and Jayanta K. Sahu. "Passively Q-switched 1.3 μm bismuth doped-fiber laser based on transition metal dichalcogenides saturable absorbers." *Optical Fiber Technology* 69 (2022): 102851. https://doi.org/10.1016/j.yofte.2022.102851
[32] Ahmad, A., M. F. A. Rahman, M. A. M. Johari, A. A. Latiff, M. H. Jali, H. H. M. Yusof, X. S. Cheng, A. R. Muhammad, and S. W. Harun. "Hafnium Bismuth Erbium Co-Doped Fiber Based Dark Pulses Generation With Black Phosphorus As Saturable Absorber." In *Journal of Physics: Conference Series*, vol. 2075, no. 1, p. 012018. IOP Publishing, 2021. https://doi.org/10.1088/1742-6596/2075/1/012018
[33] Rosol, Ahmad HA, Afiq AA Jafry, Norrima Mokhtar, Moh Yasin, and Sulaiman Wadi Harun. "Gold nanoparticles film for Q-switched pulse generation in thulium doped fiber laser cavity." *Optoelectronics Letters* 17 (2021): 449-453. https://doi.org/10.1007/s11801-021-0180-9
[34] Nayak, M. K., F. Mabood, Iskander Tlili, A. S. Dogonchi, and W. A. Khan. "Entropy optimization analysis on nonlinear thermal radiative electromagnetic Darcy–Forchheimer flow of SWCNT/MWCNT nanomaterials." *Applied Nanoscience* 11 (2021): 399-418. https://doi.org/10.1007/s13204-020-01611-8
[35] Burdanova, Maria G., Gleb M. Katyba, Reza Kashtiban, Gennady A. Komandin, Edward Butler-Caddle, Michael Staniforth, Aram A. Mkrtchyan *et al.,* "Ultrafast, high modulation depth terahertz modulators based on carbon nanotube thin films." *Carbon* 173 (2021): 245-252. https://doi.org/10.1016/j.carbon.2020.11.008
[36] Rai, D. P., Y. T. Singh, B. Chettri, M. Houmad, and P. K. Patra. "A theoretical investigation of electronic and optical properties of (6, 1) single-wall carbon nanotube (SWCNT)." *Carbon Letters* 31, no. 3 (2021): 441-448. https://doi.org/10.1007/s42823-020-00172-8
[37] Lee, J., I. Hong, and J. H. Lee. "Numerical study on an optimum Q-switching profile for complete multipeak suppression in an actively Q-switched Ytterbium fibre laser." *Laser Physics Letters* 18, no. 8 (2021): 085101. https://doi.org/10.1088/1612-202X/ac0916
[38] Rafique, Md Zubair Ebne, Ali Basiri, Jing Bai, Jiawei Zuo, and Yu Yao. "Graphene-plasmonic hybrid metasurface saturable absorber." In *Novel Optical Materials and Applications*, pp. NoM5B-3. Optica Publishing Group, 2021. https://doi.org/10.1364/NOMA.2021.NoM5B.3
[39] Yamashita, Mikio, Hiroyasu Sone, Ryuji Morita, and Hidemi Shigekawa. "Generation of monocycle-like optical pulses using induced-phase modulation between two-color femtosecond pulses with carrier phase locking." *IEEE journal of quantum electronics* 34, no. 11 (1998): 2145-2149. https://doi.org/10.1109/3.726607
[40] Fukushima, Koken, Makoto Okano, Atsushi Wada, Satoshi Tanaka, and Fumihiko Ito. "EDF laser displacement sensor based on bending characteristics of polarization-independent double-pass cascaded-chirped long-period fiber grating." *IEICE Electronics Express* 20, no. 2 (2023): 20220496-20220496. https://doi.org/10.1587/elex.19.20220496
[41] Tsallis, Constantino, FC Sa Barreto, and Edwin D. Loh. "Generalization of the Planck radiation law and application to the cosmic microwave background radiation." *Physical Review E* 52, no. 2 (1995): 1447. https://doi.org/10.1103/PhysRevE.52.1447
[42] Nady, A., Mahmoud Hazzaa M. Ahmed, Anas Abdul Latiff, Arshid Numan, CH Raymond Ooi, and Sulaiman Wadi Harun. "Nickel oxide nanoparticles as a saturable absorber for an all-fiber passively Q-switched erbium-doped fiber laser." *Laser physics* 27, no. 6 (2017): 065105. https://doi.org/10.1088/1555-6611/aa6bd7
[43] Finger, Johannes, Benedikt Bornschlegel, Martin Reininghaus, Andreas Dohrn, Markus Nießen, Arnold Gillner, and Reinhart Poprawe. "Heat input and accumulation for ultrashort pulse processing with high average power." *Advanced Optical Technologies* 7, no. 3 (2018): 145-155. https://doi.org/10.1515/aot-2018-0008